

## Beach Processes of Shirarahama "a Pocket Beach"

By Yoshito TSUCHIYA, Yoshiaki KAWATA, Teruo SHIBANO, Shigehisa NAKAMURA  
Takao YAMASHITA, Hiroshi YOSHIOKA, Shigeatsu SERIZAWA and KARDANA\*

(Manuscript received October, 5 1978)

### Abstract

The objective of this paper is to make clear the mechanics of sand transport in Shirarahama "a pocket beach" in order to study beach processes of stable, natural sandy beaches. Seasonal changes of the beach are caused by incoming waves and by blown sands, but a little beach erosion has gradually occurred due to a lack of beach sediment by recent urbanization of the hinterland. Characteristics of the change in the beach sediment are made clear, together with the present situation of the main sources of beach sediment. A method for the prediction of beach change by blown sands is proposed on the basis of both the law of sediment transport and the equation of continuity for beach changes. Changes in the distribution of longshore wave energy flux along the shoreline instead of the total rate of sand drift are considered for long-term and short-term beach changes. It is concluded from this that this beach is stable for most of the year, but the beach sediment may be transported in the offshore direction at the both ends of the pocket beach for a very short period by high waves associated with typhoons and monsoons.

### 1. Introduction

It is important in studying how to prevent beaches from erosion to make clear natural shape of stable sandy beaches which are normally located between two headlands. Such a sandy beach is called a pocket beach from the view point of the mechanics of sediment transport in the beach. R. Silvester<sup>1)</sup> proposed a headland defense work for protection of sandy beaches with erosion problems, probably based on properties of the naturally stable sandy beach. Recently, an offshore breakwater system has been fashionable in Japan<sup>2)</sup> for prevention of beaches from erosion. This system is probably similar to the headland defense work in the sense of controlling beaches. In order to consider their performances and establish their design criteria, it is necessary to make clear the beach processes of a pocket beach on the basis of observed data of the naturally stable sandy beaches.

The purpose of the present paper is to make clear the mechanics of sand transport in such a pocket beach. Shirarahama beach is fortunately one of the most typical pocket beaches in Japan. As is seen in Fig. 1, this beach belongs to

\* Coastal Engineer, Institute of Hydraulic Engineering, Bandung, Indonesia.

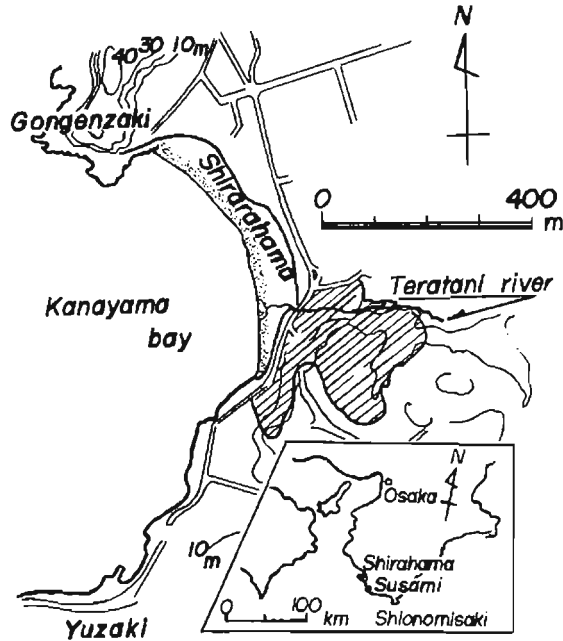


Fig. 1. Locations of Shirarahama beach and its area of sediment source.

Kanayama bay and is located between the two headlands of Yuzaki and Gongenzaki respectively. The length of this sandy beach is about 450 m along the shoreline, and the width is approximately 50 m. The present area of the back shore is estimated to be approximately 25,000 m<sup>2</sup>. Two main natural forces, such as winds and waves are predominant in the beach processes. As the beach is facing the Pacific Ocean through the Kii channel, high waves come to the beach during stormy conditions such as typhoons in the summer season as well as by monsoons in the winter season. It may therefore be expected that there are two typical changes in the beach processes caused by blown sands owing to strong winds and by sand transport owing to high waves and nearshore currents.

Due to recent urbanization of the hinterland beach erosion has gradually increased at Shirarahama beach. Continuous survey and observation have been carried out by the authors since 1970, in order to consider the two processes in the beach change. In this paper, considerations are made on the beach processes of the pocket beach, based on observed data and a few numerical simulations of the beach changes.

## 2. Characteristics of Winds, Waves and Currents

In order to investigate the beach processes, characteristics of winds, waves and

currents should first of all be considered from the observed data at the location. No wave observation has unfortunately been yet carried out off Shirarahama beach, but continuous wave observations have been made at the Shirarahama Oceanic Tower Station, Disaster Prevention Research Institute, Kyoto University which is located at a distance of a few kilometers north, and at the Susami Fishery Harbour which is located at a distance of a few tenth kilometers south. However, the data observed at the Tower Station may not be pertinent to this purpose because of the effect of locality on the wave data, so that the data observed at the harbour are used. Data observed at other locations along the Kii peninsula are also used for comparison. General characteristics of winds are considered using the wind data observed at the Tower Station and the Tanabe Fishery Office which is located at a distance of about five kilometers north. For prediction of beach change by blown sands, detailed observations of winds were carried out on Shirarahama beach.

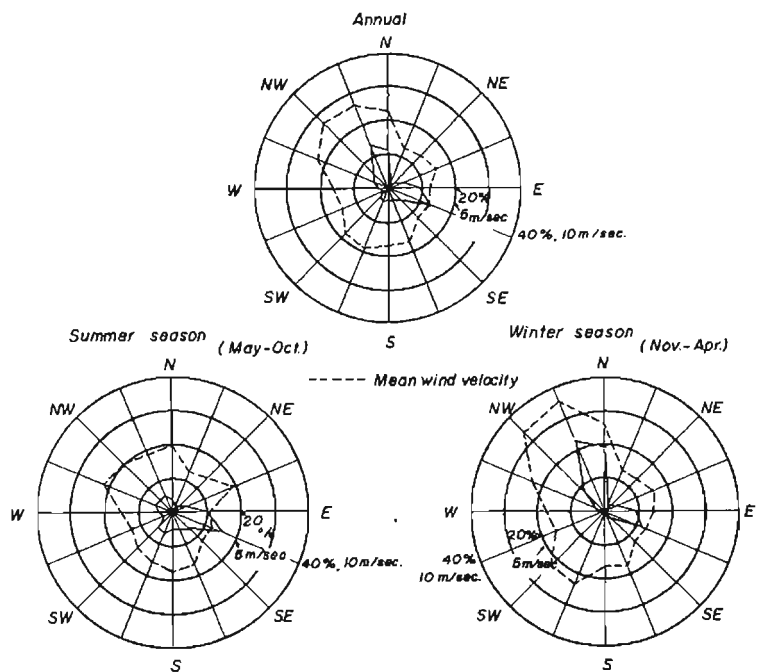
## 2.1 Winds

Characteristics of winds at the Tower Station and the Tanabe Fishery Office are plotted respectively as their wind roses in Fig. 2, in which the upper figures at these wind roses were obtained from the annual data, and the others from the summer (May to October) and winter (November to April) seasons respectively. In this figure, the dotted lines indicate the wind roses of mean wind velocity, and the solid ones those of winds stronger than 5 m/sec in velocity. The wind data of the periods between September, 1975 and August, 1976, and between July, 1974 and June, 1977 were used at the Tower Station and the Tanabe Fishery Office respectively.

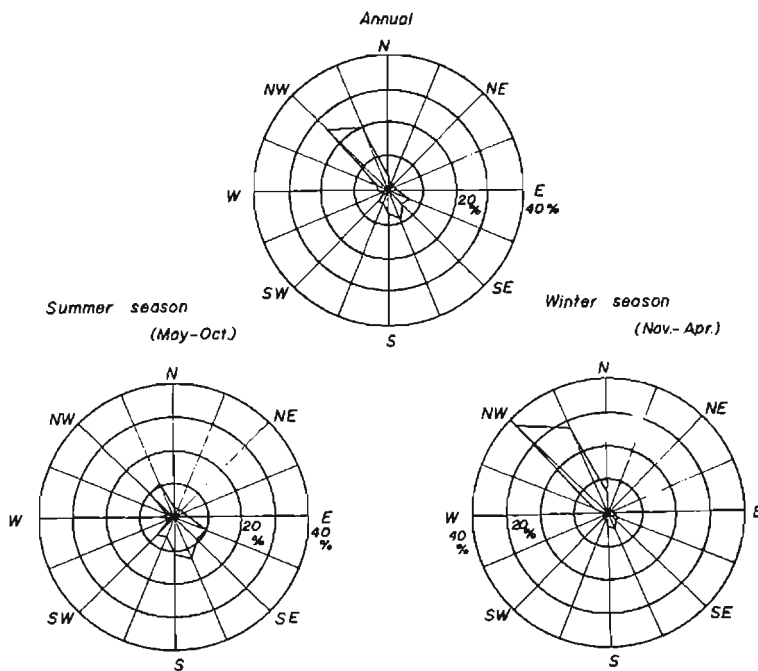
Owing to the locality of these locations, wind characteristics are different, but it is noted that the ESE winds during summer season and the NNW winds during winter season are predominant at the Tower Station, and the SSE winds during summer season and the NW wind during winter season are predominant at the Tanabe Fishery Office respectively. It may be concluded that the NW or NNW winds are predominant at Shirarahama beach owing to the monsoons in the winter season, and the predominant winds depend on the course of typhoons during the summer season.

## 2.2 Waves and Currents

As continuous wave observations have been carried out at the Shirahama Oceanic Tower Station since 1963, no observations of incident angle of waves have been made, and only a few of the observed data have been analysed. In addition, the locality of the Tower Station prevents the applicability of the data especially in stormy conditions during typhoons. The wave data are used at the Susami Fishery Harbour as shown in Fig. 3, in order to estimate the long-term beach change as well as the short-term beach change by typhoons.



(a) At Shirarahama Oceanic Tower Station.



(b) At Tanabe Fishery Office.

Fig. 2. Wind roses in vicinity of Shirarahama beach.

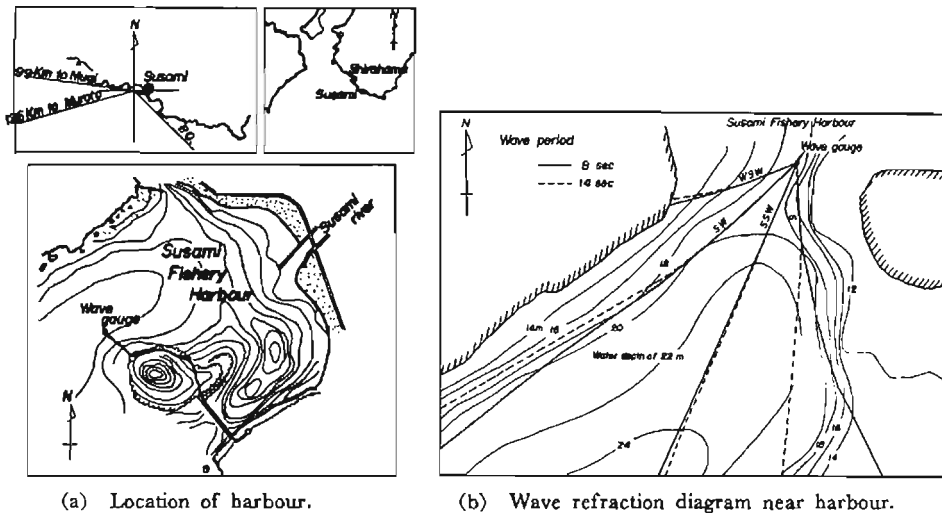


Fig. 3. Location of Susami Fishery Harbour and wave refraction diagram.

(1) Characteristics of incoming waves

Fig. 4 shows changes of monthly averaged wave height and wave period of significant waves at the fishery harbour, in which the solid lines indicate the monthly averaged wave height and the dotted ones the corresponding wave periods. The wave data observed in the period between 1965 and 1972 are used in the figure. As the harbour is located as in Fig. 3, it can not be expected to find characteristics of waves incoming to Shirarahama beach in monsoon seasons from the wave data observed at the fishery harbour. It is therefore seen that the averaged wave height increases in the summer season owing to typhoons, but does not increase in the winter season due to the locality of the harbour. It may be really expected that high waves come to the beach in the winter season due to heavy monsoon winds from the W to NNW directions. For the present purpose, characteristics of the waves incoming to the beach in the winter season should be estimated by the usual method of prediction of waves

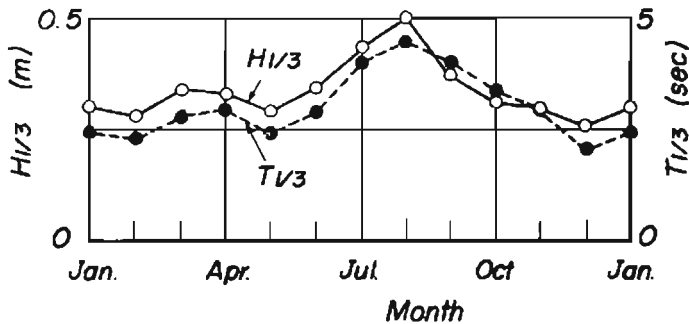


Fig. 4. Change of monthly averaged wave height and period of significant waves at Susami Fishery Harbour.

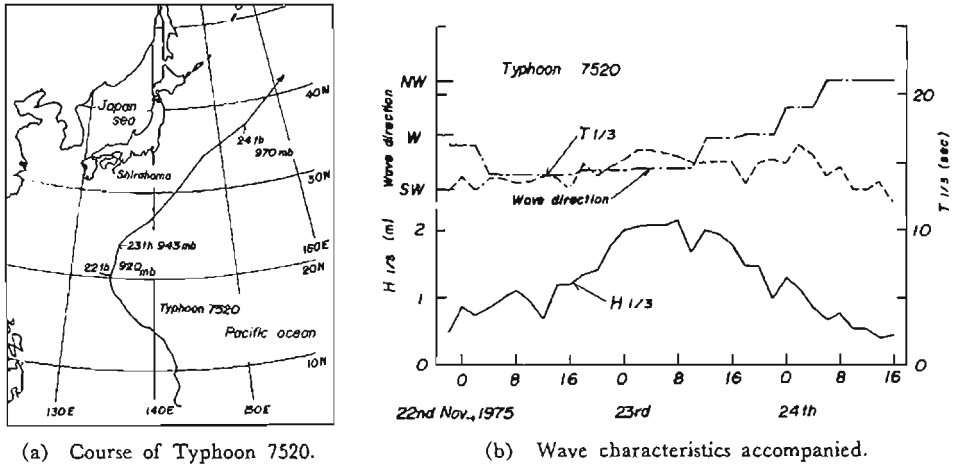


Fig. 5. Hourly changes of characteristics of waves accompanied by Typhoon 7520 at Susami Fishery Harbour.

using the wind data. It is however expected that the wave data are available in the summer season to estimate the characteristics of waves caused by typhoons, as the harbour entrance is facing the Pacific Ocean in the SW to SE directions. Necessary correction in the estimation of the incident angle of waves in deep water must be made by the wave refraction diagram in the vicinity of the harbour.

With regard to hourly changes of wave characteristics, one of the data observed at the fishery harbour is shown in Fig. 5 which was associated with the typhoon 7520. In the figure, the left figure shows the course of the typhoon and the right the changes of wave characteristics such as wave height and period of significant waves

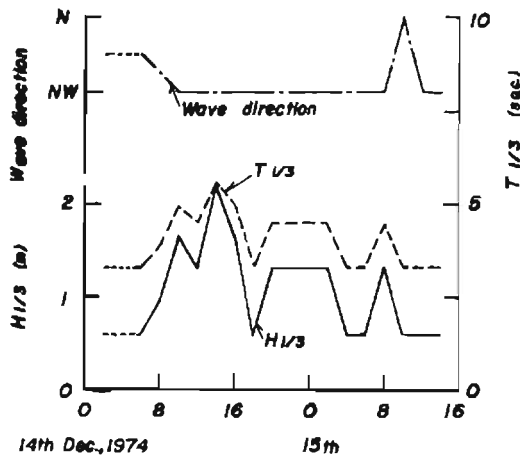


Fig. 6. Hourly changes of estimated characteristics of waves caused by monsoons off Shirarahama beach.

and wave direction. The wave directions were corrected by the wave refraction diagram shown in Fig. 3(b), to be those in deep water. It can be seen that, in this case the wave periods are 12 sec to 16 sec, the wave height is 2.14 m at maximum, and the wave direction changes to the SW direction with an approaching typhoon to Japan island and to the NW direction when it veers away from Japan. It is therefore noted that both the wave height and direction change greatly with time with the waves caused by typhoons. This fact may have great influence to the beach change.

Another example of the hourly changes in wave characteristics is shown in Fig. 6, which was estimated by the SMB method, using the wind data at the Tanabe Fishery Office in the monsoon dated in the figure. It is seen from the comparison between Figs. 5(b) and 6 that the wave heights in the monsoon are nearly the same as those in the typhoon, but the wave direction becomes predominantly NW which is dependent on the wind characteristics in the monsoon.

#### (2) Wave transformation near Shirarahama beach

In order to estimate wave characteristics near the beach, transformation of waves should be considered. The bottom configuration in Kanayama bay is very complex, especially near the headlands as is seen in Fig. 7 in which the datum T. P. +0 m corresponds nearly to the mean sealevel in this area. Wave refraction diagrams are

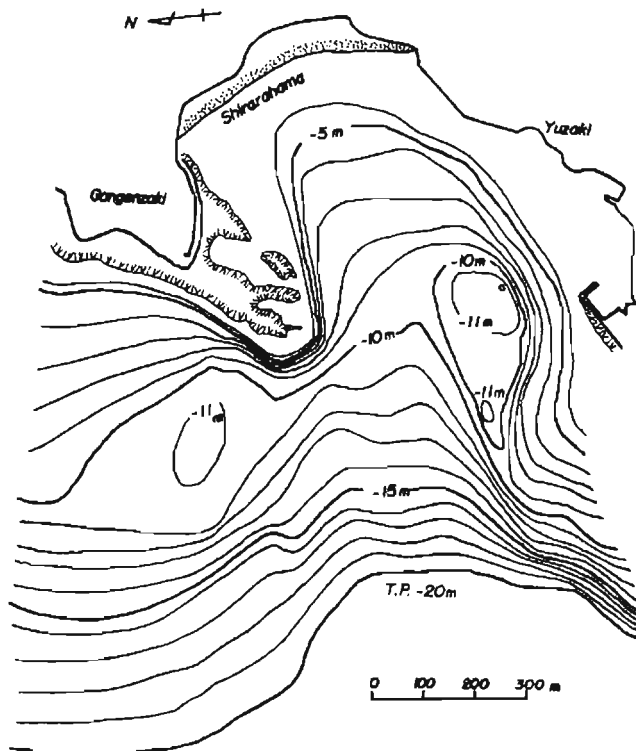


Fig. 7. Sounding chart of Kanayama bay, Shirahama.

shown in Figs. 8 and 9, which were calculated by the normal method of wave refraction with a computer. The wave refraction diagrams shown in Fig. 8 correspond to the incoming waves caused by typhoons in the summer season, and those in Fig. 9 correspond to the waves by monsoons in the winter season. As the tidal range in this

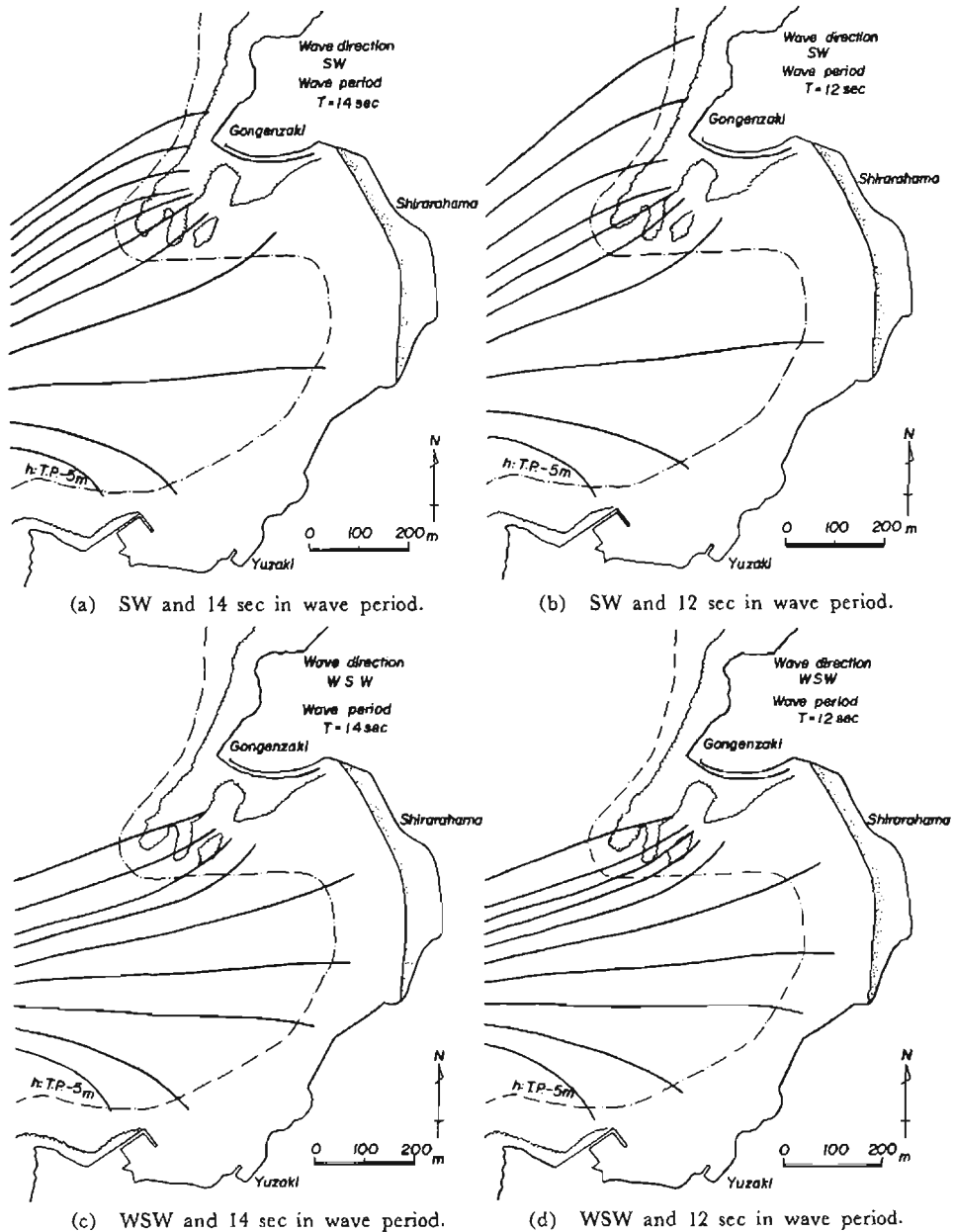
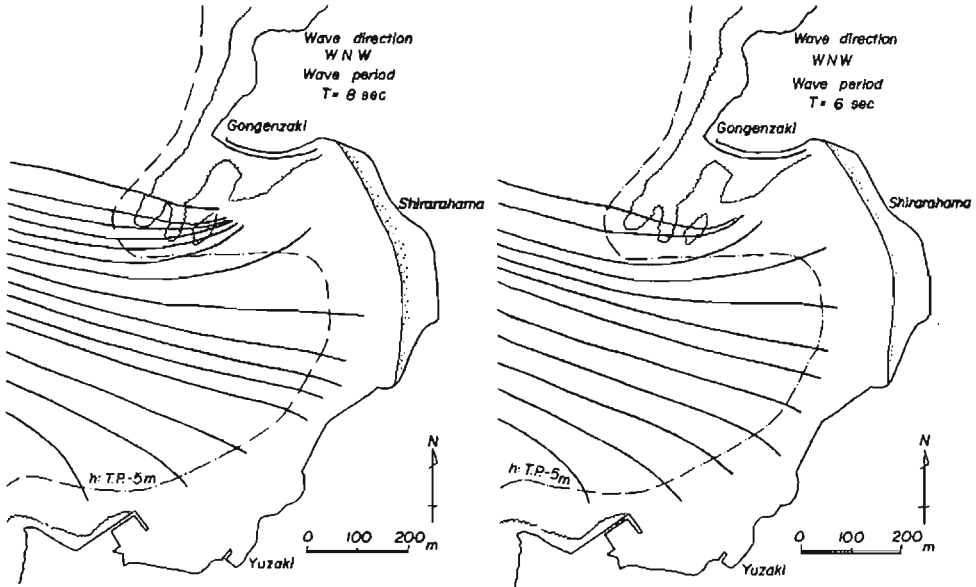


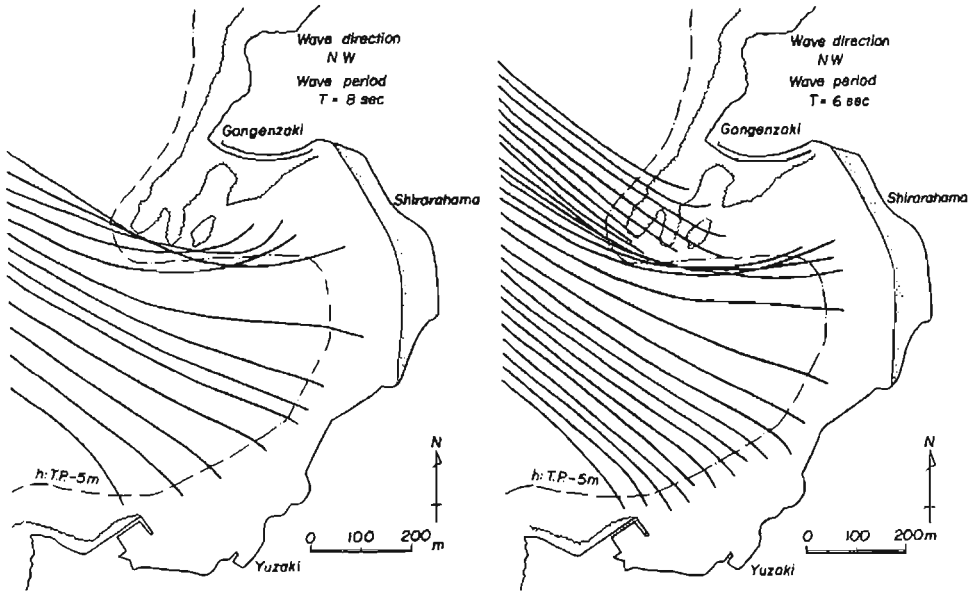
Fig. 8. Wave refraction diagrams in the case of typhoons.





(a) WNW and 8 sec in wave period.

(b) WNW and 6 sec in wave period.



(c) NW and 8 sec in wave period.

(d) NW and 6 sec in wave period.

Fig. 9. Wave refraction diagrams in the case of monsoons.

area is approximately 2.1 m at maximum, the water depth below the mean sealevel was used in the calculation of the wave refraction diagram. It can be seen for the waves in the winter season that waves coming from the NW direction concentrate near the Gongenzaki headland increasing their wave heights, but diverge at the center of the beach, which decreases them, and on the contrary the waves from the W direction come directly to the beach. It can also be considered for the waves in the summer season that the longer period waves caused by typhoons from the SW and WSW directions decrease in their wave heights owing to the wave refraction.

In addition, further considerations should be made on the wave diffraction by the headlands, as well as the effect of bottom friction on wave damping. In the evaluation of wave energy flux which is related to the rate of littoral sand drift, however, only the wave transformation due to wave refraction is taken into consideration in the last chapter.

### (3) Nearshore currents

No systematic observation of nearshore currents has yet been carried out, though it should be very important in considering the beach processes. An observation of current direction was made off Yuzaki for one year starting from January, 1976. This observation was performed twice a day at fixed times in stormy conditions. Fig. 10 shows the monthly changes in the occurrence frequencies of nearshore current direction, in which the upper and lower lines indicate the counterclockwise and clockwise directions of currents. It may be seen that the nearshore currents of counterclockwise direction are more predominant than those of clockwise ones at this position, which may be explained by the wave characteristics in stormy conditions. Some additional data observed for two months starting from 1st November, 1972 are shown in

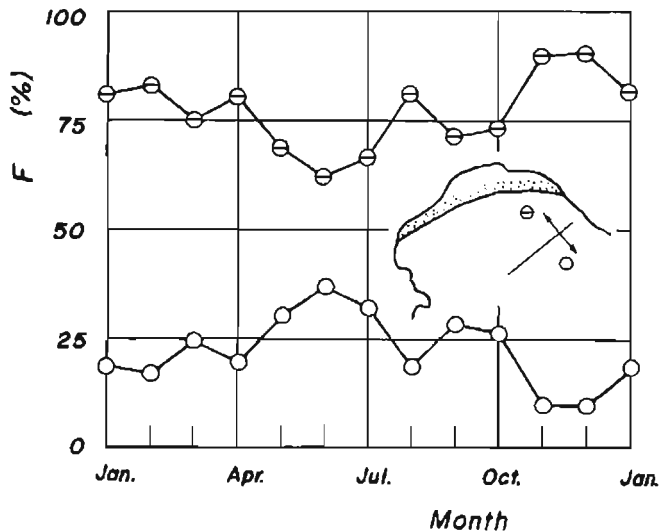


Fig. 10. Monthly changes in frequencies of direction of nearshore currents.

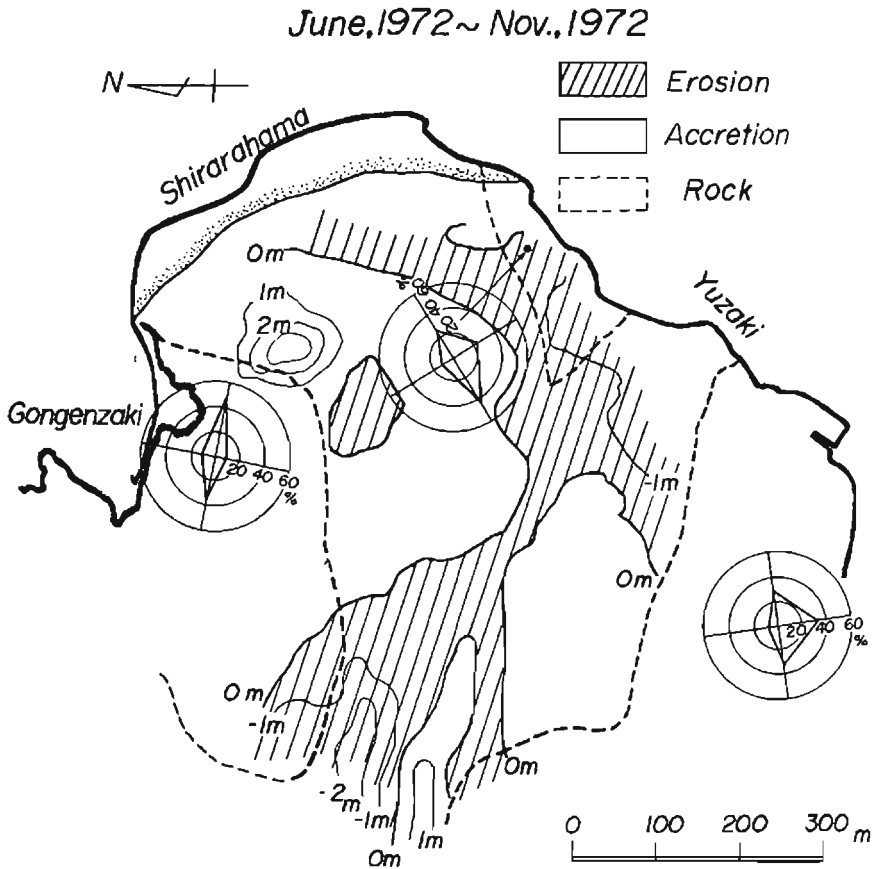


Fig. 11. Distribution of direction of nearshore currents and areas of erosion and accretion in Kanayama bay.

Fig. 11, together with the areas of erosion and accretion in Kanayama bay. It is also found that clockwise nearshore currents are predominant in the winter season, owing to the monsoon waves from the W or NW directions.

### 3. Sources and Characteristics of Beach Sediment

#### 3.1 Sources of Beach Sediment

In order to predict beach processes, the sources of beach sediment of the beach should be clarified. In this case, two probable factors are picked out as the main sources of beach sediment at Shirarahama beach. The first is the littoral sand transport along Kanayama bay through the headlands, and the second is the sand supply from the rivers located in its hinterland. It was found by the results of the sediment sampling and analysis of the adjacent beaches that no beaches have the

same sediment as Shirarahama beach has. Furthermore it was found by the sediment sampling and analysis of Kanayama bay that white sand, which is the same as that of Shirarahama, accumulates in the sunken places off the Gongenzaki headland. Needless to say, it is necessary to find the route of transportation of this white sand. Judging from the facts that the white sand has a nearly uniform distribution in size and doesn't contain any gravel, it can be assumed that the white sand was not made from the bed rock of Kanayama bay by wave action.

On the other hand, it was found by the hinterland survey that the mineral composition of the white sand is sandstone of Kanayama beds which are of uniform quality and efflorescent. The white sand is distributed within the shaded area in Fig. 1. In this figure the numbers 1, 2 and 3 indicate the positions where the sampling and analysis of sediment were carried out. Fig. 12 shows the frequency distribution of the sediment of Shirarahama beach, the bed of Kanayama bay and the Teratani river, which is the sole river running into Kanayama bay.

Fig. 13 shows the diagram of mineral composition of 22 sampling points, including those at the Teratani river, Kanayama bay and Shirarahama beach, which are classified into three groups, quartz, feldspar and other materials, which are largely pieces of broken shells. In this figure, sediment of the sampling point I was unable to analyze the sediment of the sampling point, as it was muck.

Fig. 14 shows the offshore change of the composition of quartz and feldspar along the a-a line shown in Fig. 12. It can be seen from this figure that the ratio of quartz and feldspar content exceeds ninety percent on the hinterland hill which is regarded as the source of beach sediment, while in Kanayama bay its ratio decreases with the distance from the shoreline, but the ratio of feldspar content nearly is constant in the offshore direction. It can be considered that the high quartz content makes

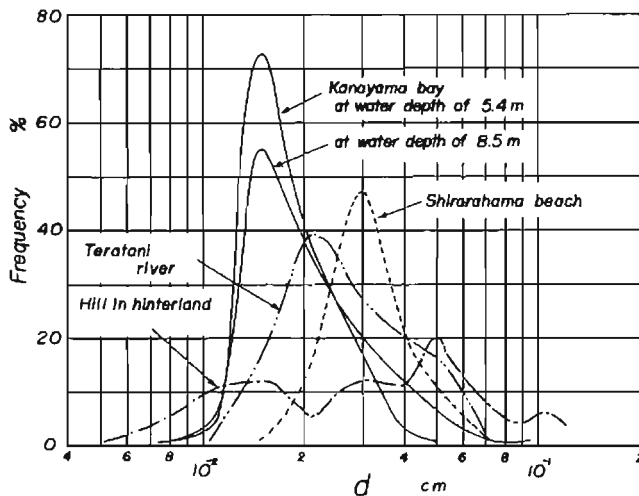


Fig. 12. Frequency distributions of sediment at Teratani river, Shirarahama beach and Kanayama bay.

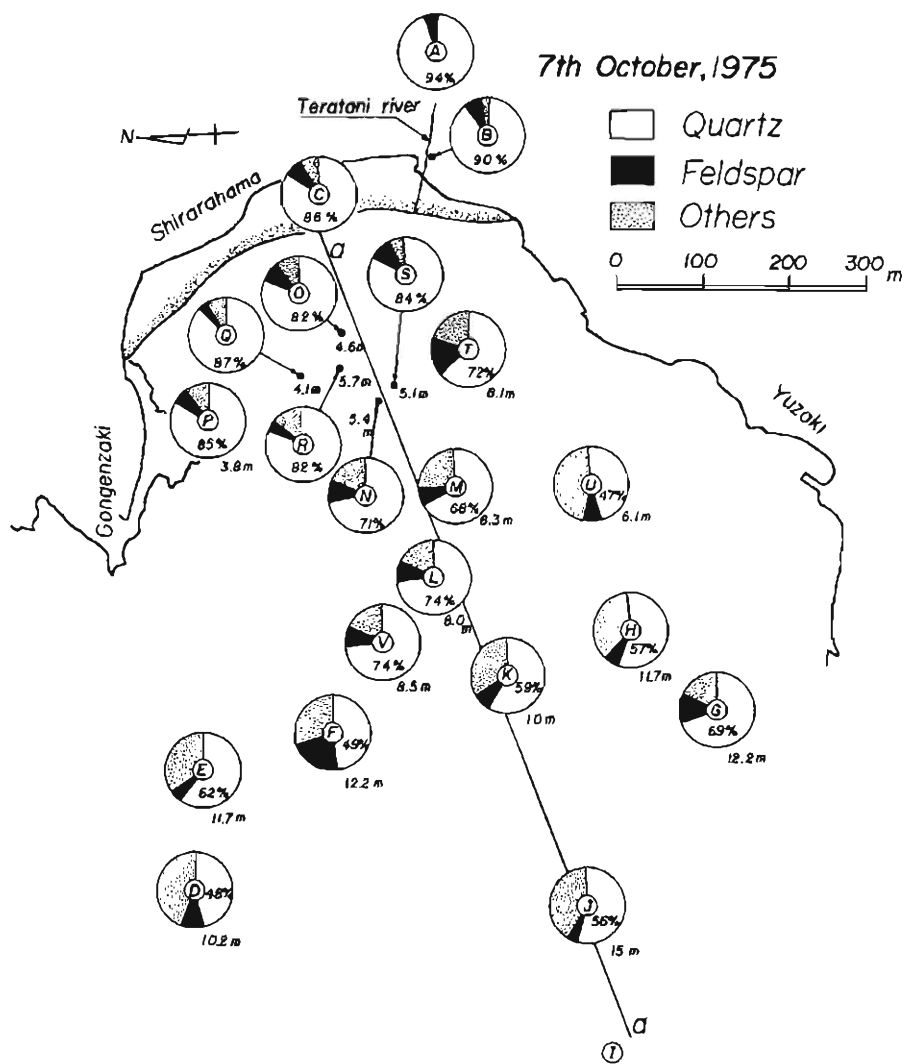


Fig. 19. Areal distribution of mineral composition on and off Shirarahama beach.

Shirarahama beach white and the decreasing tendency of quartz with distance makes the color of the sediment change to brown.

And Fig. 15 shows the areal distribution of median diameter of the bottom sediment in Kanayama bay by thick, solid lines, together with contour lines of water depth indicated by the thin solid lines. The sediment were sampled in small holes on the rocky bed more offshore than the water depth of about ten meters. It was seen that there exists a little white sand in the small holes, whose size decreases gradually in the offshore direction, but increases slightly in the more offshore area, which may be due to the effect of wave action. Although it has not been made clear

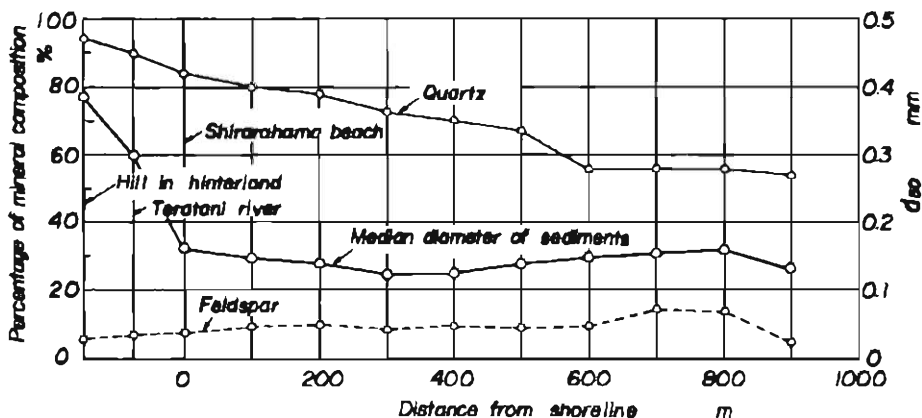


Fig. 14. Offshore changes of median diameter of bottom sediment and their composition of quartz and feldspar.

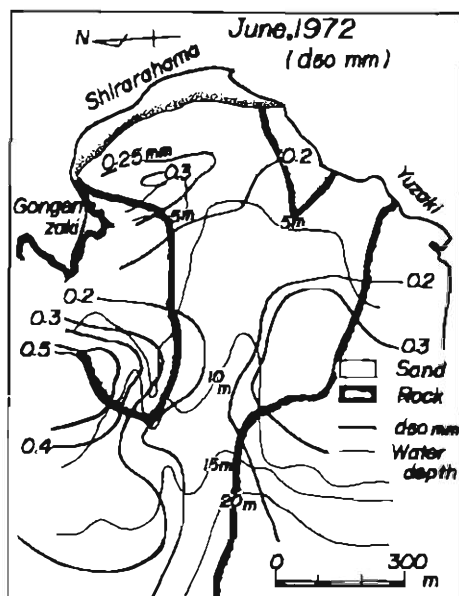


Fig. 15. Areal distribution of median diameter of bottom sediment in Kanayama bay.

whether the white sediment is transported from the beach or not, the sediment probably is the same one as that on the beach as they both have nearly the same size and quality.

From the facts described above it may be concluded that the sources of Shirarahama's white sand should be the hinterland hill of which area is shown in Fig. 1. It is however difficult to conclude that Shirarahama beach was formed only with the bed load transported from the Teratani river as it is a very small river. It

is natural to consider that the white sand was supplied by erosion of the hinterland hill before the urbanization of the present Shirahama-cho. It should be taken into consideration in studying the beach processes that the input of the white sediment both from the hinterland and the Teratani river has decreased recently due to urbanization.

### 3.2 Characteristics of Beach Sediment

In order to make clear the areal distribution of beach sediment on Shirahama beach, sampling of sediment was carried out at and along the shoreline at intervals of one hour from 8:00 which is high tide, to 14:00 which is low tide, on 13th March, 1978, the time of the spring tide.

Fig. 16 shows the areal distribution of the median diameter of sediment with contours, in which the small black circles indicate the position of sediment sampling. Fig. 17 also shows the areal distribution of the standard deviation of beach sediment. As is seen in Fig. 16, the distribution of median diameter has a tendency of rhythmic change alongshore so that the region of large diameter of sediment appears at the intervals of about seventy to eighty meters at the stage of high and low tides. Moreover the median diameter of sediment at the southern part of the beach is nearly 0.6 mm to 0.7 mm which are slightly larger than that at the other part. Nearly the same tendencies can be found in the distribution of the standard deviation of beach sediment as shown in Fig. 17.

Judging from the fact that the parts of large median diameters and of lowsorting sediment appear at intervals of about seventy to eighty meters, it is considered that the beach cusps on the beach appear at the same intervals.

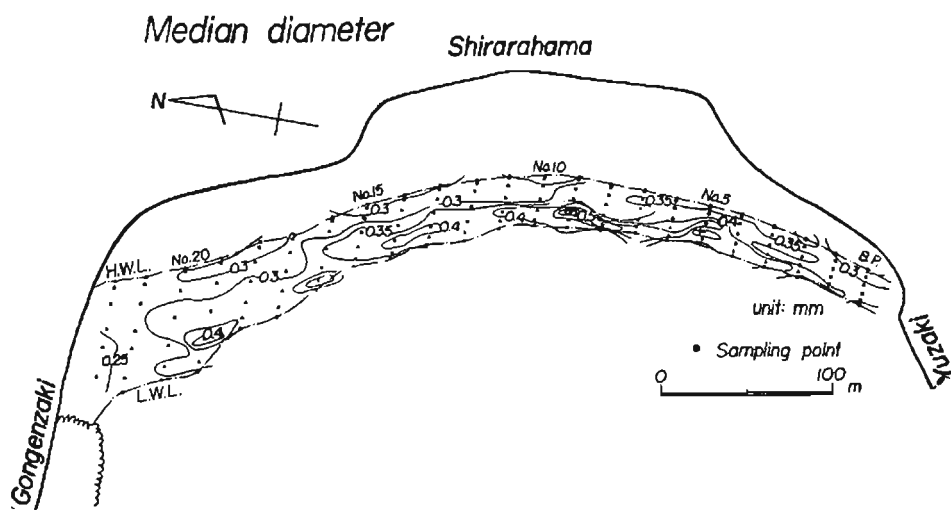


Fig. 16. Areal distribution of median diameter of beach sediment.

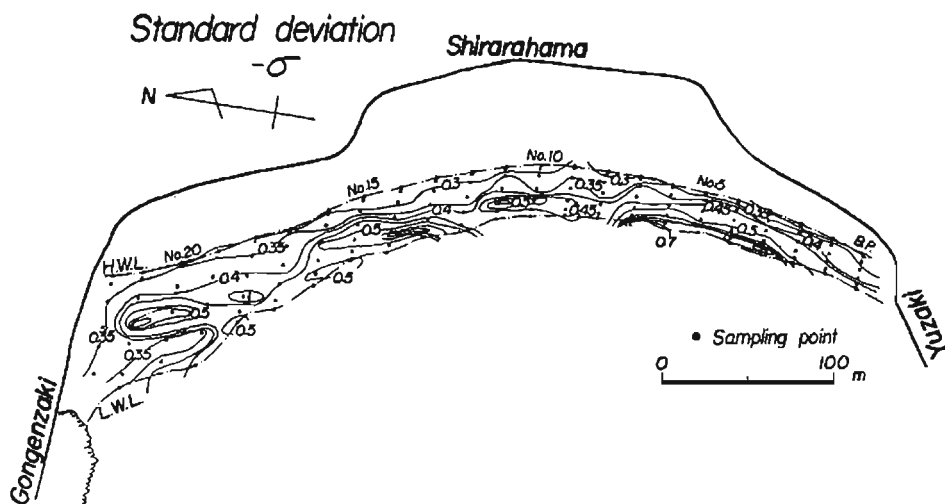


Fig. 17. Areal distribution of standard deviation of beach sediment.

Diameters and standard deviations of the beach sediment along the temporary shoreline which were taken at the interval of one hour are shown in Fig. 18, in which  $d_{50}$  is the median diameter,  $d_{95}$  the diameter of 95 percentile of sediment sample and  $\sigma_\phi$  the standard deviation in the phi scale. In the figure, the distance is taken from the point of B. P. shown in Figs. 16 and 17, and the arrows indicate predominant directions of littoral sand drift which are estimated by decreasing or increasing tendencies in the diameters and standard deviation respectively. The distributions at the highest water level which is usually considered to be the run-up limit of high waves, the high water level of usual tides and the run-up height which is influenced by usual waves are shown in Fig. 18(a), (b) and (c) respectively. In these figures the longshore peaks of the median diameter appear at different points. In the upper and lower figures, the peaks appear at the distance of 150 m to 200 m from the point of B. P. shown in Figs. 16 and 17, and the peak values gradually decrease, but the standard deviations become larger at the both ends of the beach. On the contrary, in the middle figure the standard deviations become larger at the ends.

It is concluded that the longshore distributions of median diameters and standard deviations of the beach sediment at each tidal level explain well the histories of incoming waves as well as swash movement, and that the beach sediment may be transported from the central part of the beach to the both ends in this period of observations.

#### 4. Beach Change by Winds

As already mentioned, it is important to predict the beach change by winds in winter and spring seasons at Shirarahama beach. Deposition of the beach sediment



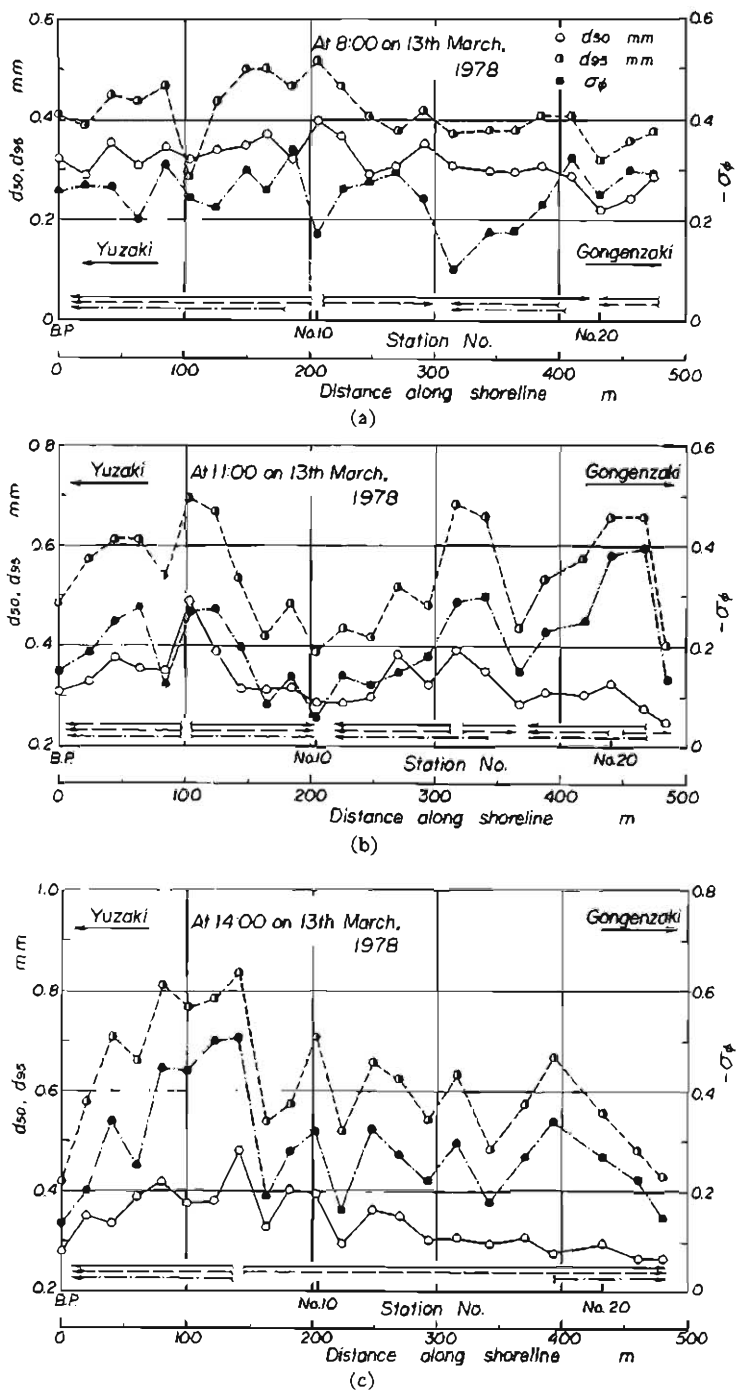


Fig. 18. Alongshore distribution of diameters and standard deviation of beach sediment at different sea levels.

occurs on the road and neighbouring area located behind the beach in the south direction, and its total volume is estimated to be several thousand cubic meters per year owing to a few monsoon winds. A method of prediction of beach change by winds is presented, based on the detailed observations of both blown sands and beach changes.

#### 4.1 Beach Change by Winds

In order to find beach processes by winds, a systematic observation of beach change had been carried out at Shirarahama beach for several years starting from 1970. Fig. 19 illustrates the beach change by winds during the periods indicated in the figure, in which the shaded and unshaded areas indicate erosion and accretion respectively, and the counterlines indicate their elevation from the reference datum line. In this figure, especially in Fig. 19(a) and (b), the beach change was considered to be due to both blown sands and waves during the winter monsoon. It can be seen that distributions of the areas of erosion and accretion are similar in these figures, such erosion and accretion occur in the northern and southern parts of the beach respectively, which are mainly caused by the NW and NNW winds during the winter season.

Fig. 19(c) shows an example of the beach changes in the spring season. It is seen that, on the contrary, the general tendency of beach change is different from that in

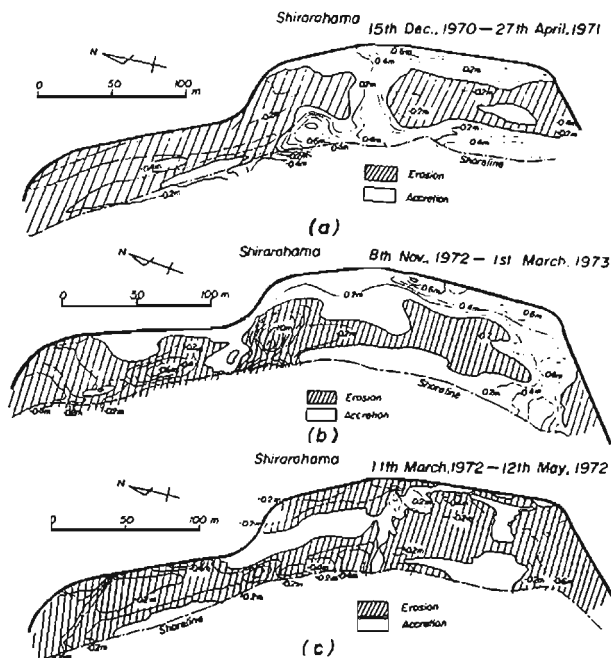


Fig. 19. Beach change in Shirarahama by wind.

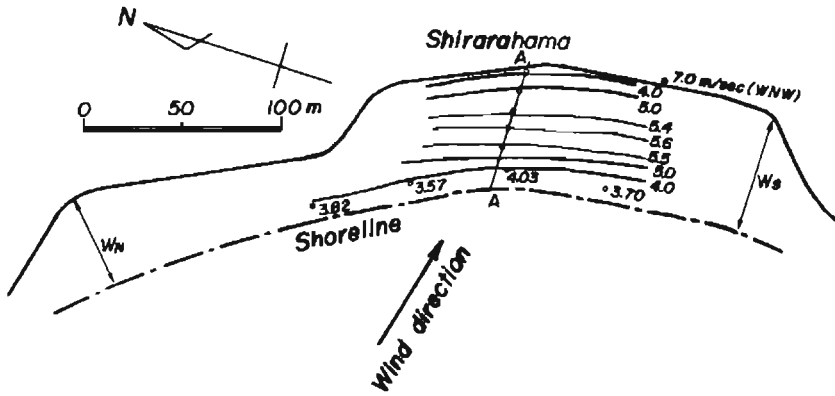


Fig. 20. Areal distribution of wind speed on Shirarahama beach in spring season.

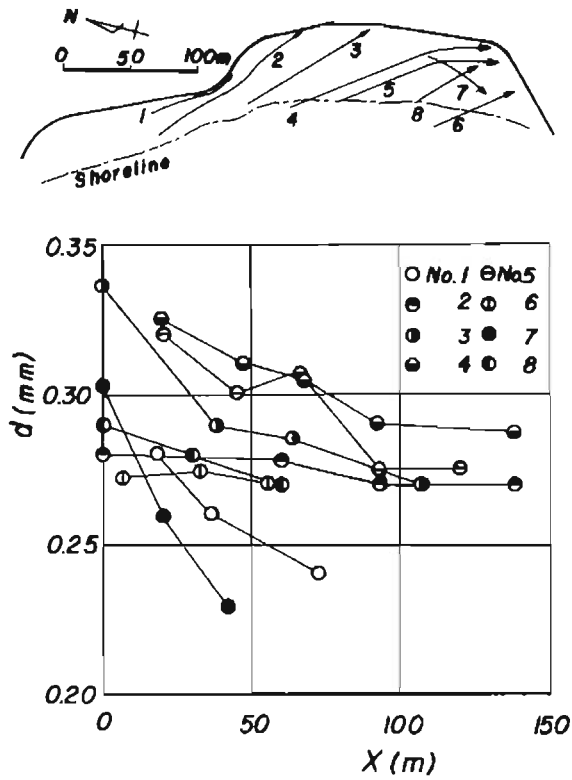


Fig. 21. Change of median diameter of surface sediment on Shirarahama beach with the distance from shoreline in predominant direction of wind.

the winter season, and that the beach change occurs in a nearly normal direction to the shoreline, especially severe erosion occurs near the front of the sea dike located just behind the beach. This may be caused both by high waves and strong winds from the W and SW directions due to abnormal low pressures. In the spring season, as part of the moved sediment overtops the sea dike to deposit on the road and adjacent area, the volume of the eroded sediments in the beach exceeds generally that of the accreted one as is seen in the figure. Fig. 20 shows one of the areal distributions of wind speed in the WNW direction in the spring season. This describes a tendency of wind speed increasing in the direction normal to the shoreline. This nearly corresponds to the general situation of the beach change near the area caused by blown sands.

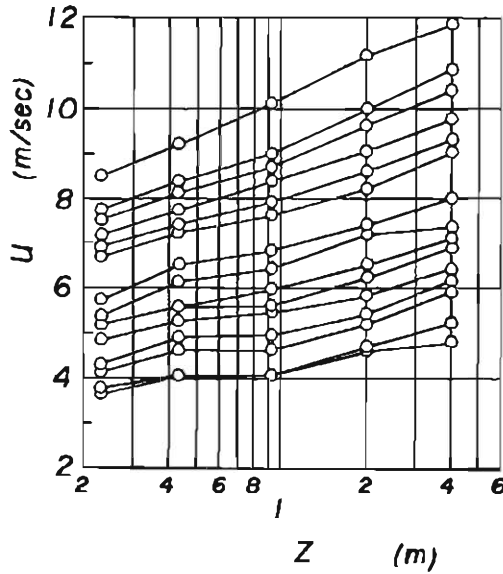
Fig. 21 describes the areal distribution of median diameter of the beach sediment which was sampled on the sand surface, in the predominant direction of winds, in which the origin is expressed at the shoreline by an arrow in the upper figure. It is seen that the median diameters of the surface sediment decrease gradually with the distance and their directions coincide with the predominant ones of winds during the strong winds.

#### 4.2 Prediction of Beach Change

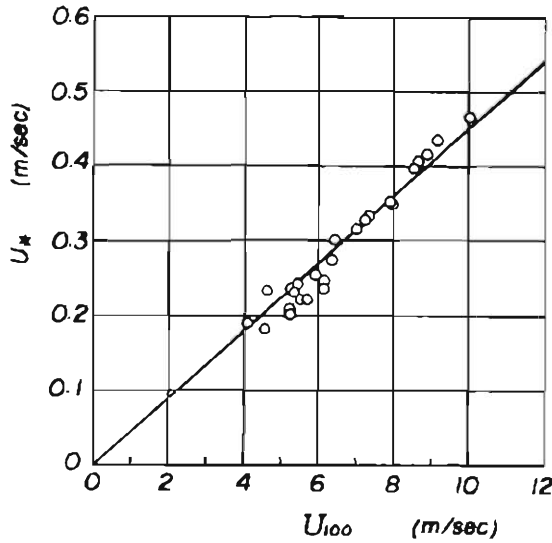
As already described, an observation was also carried out to measure the rate of sediment transport by winds on the beach with a sand trap, as well as the wind velocity with a set of five small anemometers of cup-type for the estimation of shear stress on the sand surface by wind action. The sand trap used was specially designed, based on the trap of the V-5 type proposed by Horikawa and Shen<sup>3)</sup>, the dimensions of which are 15 cm wide, 25 cm long and 30 cm high. A continuous observation of winds was performed with an anemometer of vane type at the distance of about ten meter above the mean sealevel on the sea dike.

Wind velocities observed were averaged for five minutes to evaluate the averaged wind velocity. The total rate of blown sands was measured at intervals of several minutes. A few examples of the observed wind velocities are shown in Fig. 22, in which  $u$  is the averaged wind velocity and  $z$  the vertical distance from the sand surface. The estimation of the shear stress could be made according to the normal logarithmic law of velocity profile, as is seen in Fig. 23 showing a relation between the estimated shear stress and the wind velocity at the distance of 100 cm above the sand surface.

Estimated is the shear stress from the observed wind velocity by the straight line shown in the figure. The observed data of the total rate of blown sands is shown in Fig. 23, in which the solid line indicates the theoretical law of sediment transport by winds, which was derived by Tsuchiya and Kawata<sup>4)</sup> on the basis of both the mechanics of saltation of sand grains and the conservation law of momentum in a saltation layer.



(a) Velocity profiles of winds.



(b) Relation between shear velocity and wind velocity at distance of one meter.

Fig. 22. Velocity profiles of winds and estimation of shear velocity.

It is given as

$$\begin{aligned}
 \tau^* &= 4.62 \left[ 1 + 0.495 (1 - 1.05e) \left( 1 - \frac{1}{r^2} \right)^2 \right] \\
 &\sqrt{0.0286 + 4.70 \left[ 1 + e - (1 - e) \sqrt{1 + \frac{0.355}{(1 - e)\tau^*}} \right]^2 \left( 1 - \frac{1}{r^2} \right)^2 (\tau^* - \tau_c^*)} \quad (1)
 \end{aligned}$$

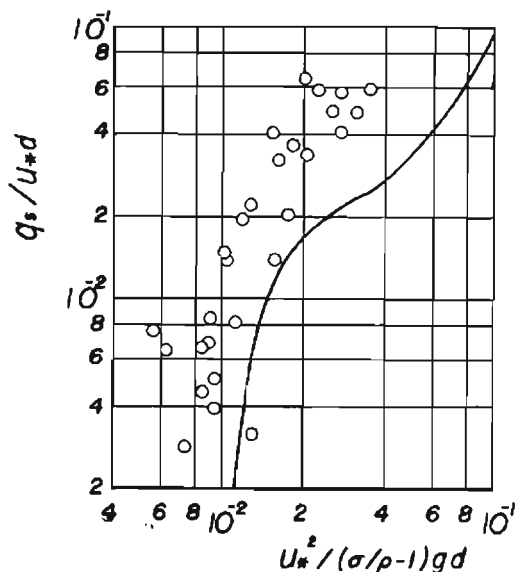


Fig. 23. Comparison between sediment transport law by wind and observed data.

in which  $q^* = q_B / u_*^2 d_{50}$ ,  $\tau^* = u_*^2 / (\sigma/\rho - 1) g d_{50}$ ,  $\tau_c^* = u_c^2 / (\sigma/\rho - 1) g d_{50}$ ,  $e = 0.95 / (1 + 5.47\tau^*)$ ,  $r = 0.95(1 + 65.0\tau^*) / (1 + 5.47\tau^*)$ ,  $q_B$  is the rate of sediment transport by winds,  $\sigma/\rho$  the relative density of sediment in air,  $g$  the acceleration of gravity,  $u^*$  the shear velocity,  $u_c^*$  the critical shear velocity for sediment threshold, and  $e$  the coefficient of rebounding of a grain. In the theoretical curve shown in the figure, it was assumed that  $\tau_c^* = 0.01$  for practical purposes. The data shown in the figure were observed for periods of more than thirty minutes. It is however seen that the observed data are generally plotted higher than the theoretical values, especially near the sediment threshold. It seems for this that the shear velocity was considerably small when estimated by the averaged wind velocity owing to the fluctuation and gust in winds, because of shorter periods of the measurement of the total rate of blown sands than those of the wind measurement.

It is necessary, on the other hand, to formulate the distribution of shear stress on the beach in predicting the beach change by winds. Fig. 24 illustrates the change of wind velocity with the distance from the shoreline in the predominant W and WNW directions, which was estimated from the velocity profiles measured, in which the thin solid lines are derived by the method of conformal mapping in the potential theory of a flow on a wedge-shaped slope with an angle corresponding to the gradient of beach slope near the shoreline. It is then expressed by

$$\frac{u_*}{U_K} = \beta \left( \frac{x}{x_0} \right)^{a/\tau} \quad (2)$$

in which  $U_K$  is the ten minutes averaged wind velocity at the anemometer of vane

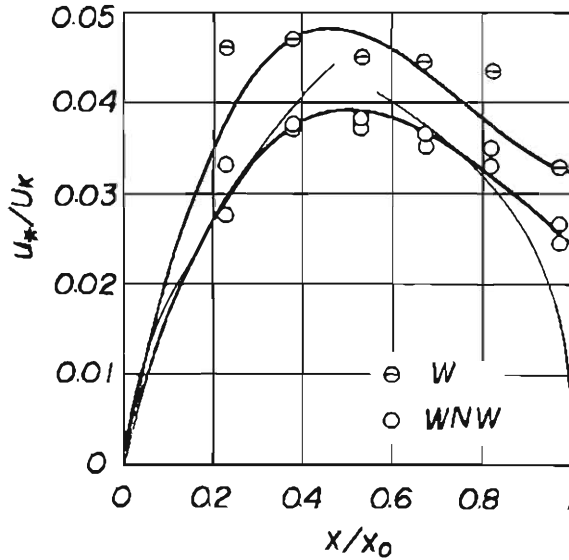


Fig. 24. Changes in wind velocity on Shirarahama beach with distance from shoreline.

type,  $x$  the distance from the shoreline in the direction of winds,  $x_0$  the distance of the beach in the same direction, and  $\beta$  a constant. It is seen that the distribution of wind velocity can be explained by the formula near the shoreline, but the distribution on the beach can not be expressed by it because of the nonuniform beach slope. An empirical formula shown in the figure by the thick solid line is applied. It is expressed by

$$\frac{u^*}{U\kappa} = a\left(\frac{x}{x_0}\right)^3 + b\left(\frac{x}{x_0}\right)^2 + c\left(\frac{x}{x_0}\right) \quad (3)$$

in which  $a=0.105$ ,  $b=-0.264$  and  $c=0.184$  for the WNW winds, and  $a=0.170$ ,  $b=-0.382$  and  $c=0.245$  for the W winds.

Let the co-ordinate be along the beach surface in the direction of winds, the equation of continuity of beach change can be expressed by the one-dimensional approach as

$$\frac{\partial \bar{z}}{\partial t} + \frac{1}{1-\lambda} \left(\frac{d_{50}}{x_0}\right) \left(\frac{\partial q_b^*}{\partial \bar{x}}\right) = 0 \quad (4)$$

in which  $\bar{z} = z/d_{50}$ ,  $l = (\sigma/\rho - 1)g/d_{50}l$ ,  $\bar{x} = x/x_0$ ,  $q_b^* = q_b/\sqrt{(\sigma/\rho - 1)gd_{50}^3}$ ,  $z$  is the vertical distance of sand surface from the datum line,  $t$  the time, and  $\lambda$  the porosity of sediment by a factor of one percent. Substitution of Eq. (1) into Eq. (4) may yield the basic equation of beach change.

Making the assumptions that the wind velocity changes gradually with time and the linear super-position of temporal beach changes can then be made, the solution of the beach change may be expressed as

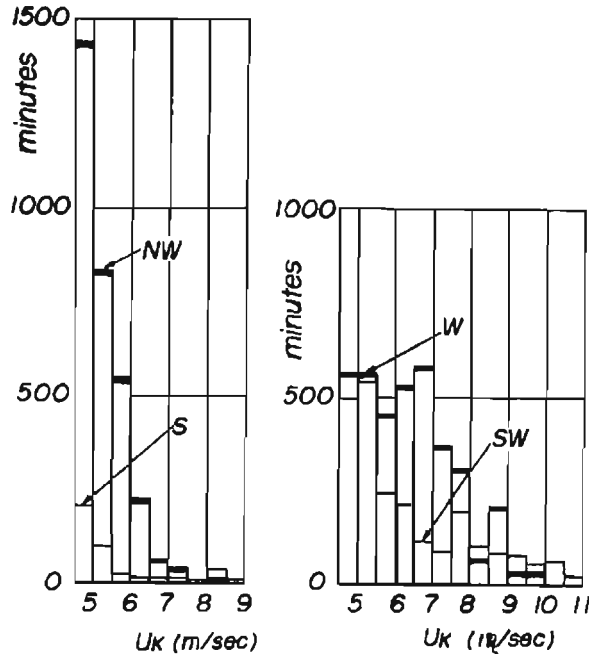


Fig. 25. Occurrence frequency of winds for the period between March and May, 1972 at Shirarahama beach.

$$\bar{z} = -\frac{1}{1-\lambda} \left( \frac{d_{\omega}}{x_0} \right) \sum_i \left( \frac{\partial q_{\beta}^*}{\partial x} \right)_i t_i \quad (5)$$

in which the suffix  $i$  indicates the interval of wind velocities.

An application of the approach is described to predict the one dimensional beach change in the predominant direction. Fig. 25 shows the occurrence total duration of winds in every wind direction for the period between March and May, 1972, in which the wind velocities shown were measured with the anemometer of vane type. Beach changes by the winds can be predicted by the linear super-position of Eq. (5) in every direction. The final result of the super-position is shown in Fig. 26, in which the thin solid lines indicated by W, NW and SW are the beach changes predicted from the W, NW and SW winds, respectively, and the total and observed beach changes are shown by the thick solid and dotted lines, respectively. The observed beach profile was measured from the beach profile averaged for the period. It can be found from the figure that most of the beach changes by winds in the spring season are caused by the W winds, and that the ranges of  $0.1 < x/x_0 < 0.5$  and  $0.5 < x/x_0 < 0.8$  are eroded and accreted respectively. It is also found that the theoretical prediction of the beach change agrees generally with the observed beach change except for the vicinity of the shoreline and the sea dike.

As an influence of the tides and wave run-up may come up to the position of  $x/x_0 = 0.12$ , the initiation of beach change by winds is assumed to be the position in



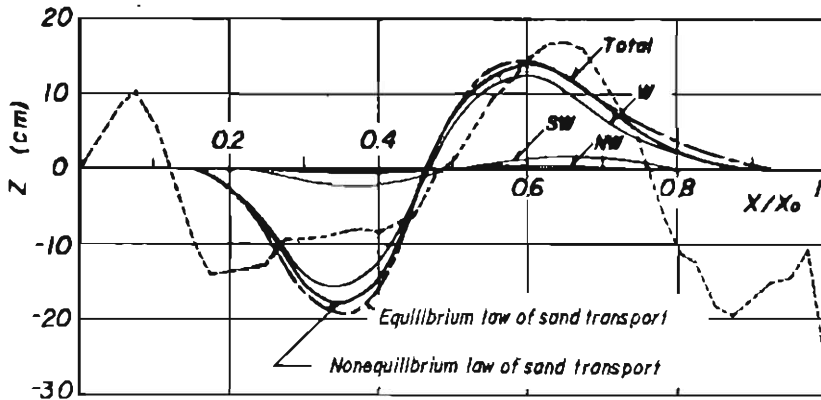


Fig. 26. Comparison between theoretical and observed beach profile changes in predominant directions for the period between March and May, 1972.

which there is a small deposition of sediment by wave run-up. It is seen that the theoretical initial point of the beach change by winds is in the vicinity of the position. For the range of  $x/x_0 > 0.8$ , on the other hand, local scour occurs near the sea dikes owing to the winds along them, so that the one-dimensional continuity of beach change may no longer be satisfied.

### 5. Beach Change by Waves

As already described, beach change had gradually occurred because of waves at Shirarahama beach, but it has not been so severe. Originally the beach was nearly stable as it is one of the pocket beaches. Owing to the recent urbanization, the sources of beach sediment have been exhausted. In order to preserve this beach, it should be very important to find main causes of the sediment output from the nearshore area by wave action. This deals probably with characteristics of such a pocket beach.

From this point of view, mechanism of sand drift in the pocket beach, where the sediment sources have been exhausted, is considered on the basis of the longshore distribution of littoral sand drift. According to Komar<sup>5)</sup>, the total rate of littoral sand drift has been reconfirmed to be formulated as

$$Q_s = 0.77 F \quad (6)$$

in which  $Q_s$  is the total rate of littoral sand drift and  $F$  the longshore component of wave energy flux being given by

$$F = \frac{1}{2} (E c_n)_b \sin 2\alpha_b \quad (7)$$

in which  $(E c_n)_b$  is the wave energy flux at the breaking point and  $\alpha_b$  the incident angle of waves at the point. More recently this formula has been theoretically derived by Tsuchiya and Yasuda<sup>6)</sup> on the basis of the mechanics of sediment transport and the

theory of longshore currents. The longshore wave energy flux is therefore applicable to estimate the longshore distribution of the total rate of littoral sand drift and to consider beach changes for practical purposes.

### 5.1 Wave Energy Flux

#### (1) Evaluation of wave energy flux

To compute wave refraction is essential in evaluating wave energy flux. A computer program of the wave refraction diagram was developed by Worthington and Herbich<sup>7)</sup> and a similar program is used to evaluate the longshore wave energy flux along Shirarahama beach. As shown in Fig. 1, there are two rocky headlands, Gongenzaki and Yuzaki, and submarine irregular rocky bottom which stretches away from these headlands to the central area of Kanayama bay, protecting the white sandy beach from direct action of high waves. Under certain wave directions and wave periods, some of the wave rays have a tendency to converge or cross each other due to the irregular bottom topography near the headlands. In this situation the distance between the adjacent wave rays decreases to become zero, and the wave height then should increase infinitely at the crossing point, but actually the breaking of waves appears. Both the wave refraction and shoaling can be calculated by this computer program. The breaker characteristics such as the breaker height, breaking depth of water and incident angle should then be calculated to estimate the wave energy flux.

For estimation of the breaking depth of water the empirical formula proposed by the Coastal Engineering Research Center<sup>10)</sup> is applicable, and it is expressed by

$$\frac{h_b}{H_b} = \frac{1}{b - (aH_b/gT^2)} \quad (8)$$

which is one of the reliable criteria of wave breaking, in which  $h_b$  is the breaking depth of water,  $H_b$  the breaker height,  $a$  and  $b$  are the functions of the beach slope  $\tan \beta$ , and are approximated by

$$a = 1.36(1 - e^{-19.6 \tan \beta}), \quad b = \frac{1.56}{1 + e^{-19.6 \tan \beta}} \quad (9)$$

As the longshore wave energy flux per unit crest length at the breaking point is expressed by Eq. (7), the total longshore wave energy flux  $F$  for a long-term period may be given by

$$F_0 = \sum_i f_i F_i \Delta t \quad (10)$$

in which  $f_i$  is the number of wave data having the same wave characteristics for a long-term period and  $\Delta t$  the duration time which corresponds to the wave measuring time interval, say two hours in this case. It is assumed that, in each wave ray, the representative wave breaking point is defined at which the waves with the highest frequency of appearance break. For estimation of the longshore wave energy flux of a series of high waves in stormy conditions, Eq. (10) is also applicable.

#### (2) Longshore distribution of wave energy flux

In order to evaluate the longshore wave energy flux for a long-term period, the wave data observed from April, 1970 to March, 1976 at the Susami Fishery Harbour were available for the summer season between May and October, and those estimated by the SMB method using the wind data measured from July, 1974 to June, 1977 at the Tanabe Fishery Office were also available for the winter season between November and April. The distribution of the longshore wave energy flux along Shirarahama beach in the summer season is shown in Fig. 27, in which the horizontal axis indicates the distance from the Yuzaki headland in the northern direction, the vertical axis the longshore wave energy flux of which direction is taken positive in the northern direction, and  $\alpha$  is the incident angle of waves in deep water. It is found in the summer season that the waves approaching from the directions that  $\alpha=90^\circ$  and  $126^\circ$  produce a lot of wave energy flux near the northern part of the beach, but the total wave energy flux has a tendency decreasing to zero at its both ends and near its central part. It should be noted that the value of the wave energy flux near the Gongenzaki headland is questionable due to the doubtful applicability of the wave breaking criterion to the irregular rocky bottom and no consideration of wave diffraction by the lee of the rocky headland.

The distribution of the longshore wave energy flux in the winter season is shown in Fig. 28. It is apparent in the winter season that northwestern monsoons are so dominant, as already described, that the distribution of the total wave energy flux are governed by the high wind waves travelling from its direction. It is, moreover, recognized that the total wave energy flux decreases to zero at the both ends of Shirarahama beach and near its central part the same as in the summer season. The distribution of the annual wave energy flux, which was evaluated by the sum of the total ones in the summer and winter seasons is shown in Fig. 29. It is concluded from this figure that the longshore wave energy flux comes to almost zero at the both

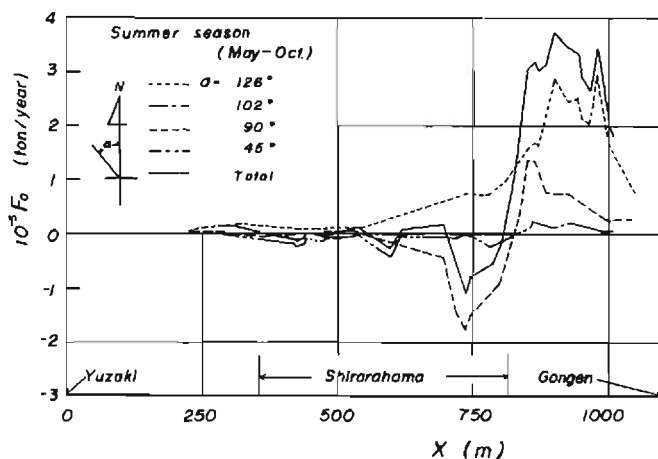


Fig. 27. Longshore distribution of wave energy flux in summer season.

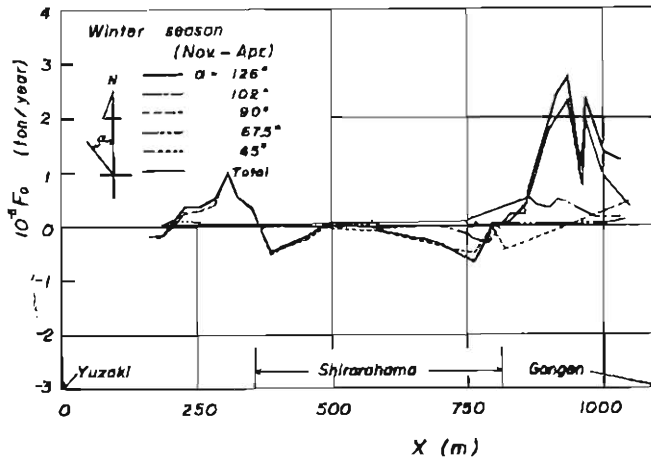


Fig. 28. Longshore distribution of wave energy flux in winter season.

ends of Shirarahama beach and near its central part. Although the wave data used are not so accurate to find the general law of the distribution of wave energy flux along a pocket beach, it may be expected that the sum of wave energy flux decreases to zero at the both ends of stable pocket beaches. It should therefore be necessary to confirm this fact by some other stable pocket beaches for this purpose.

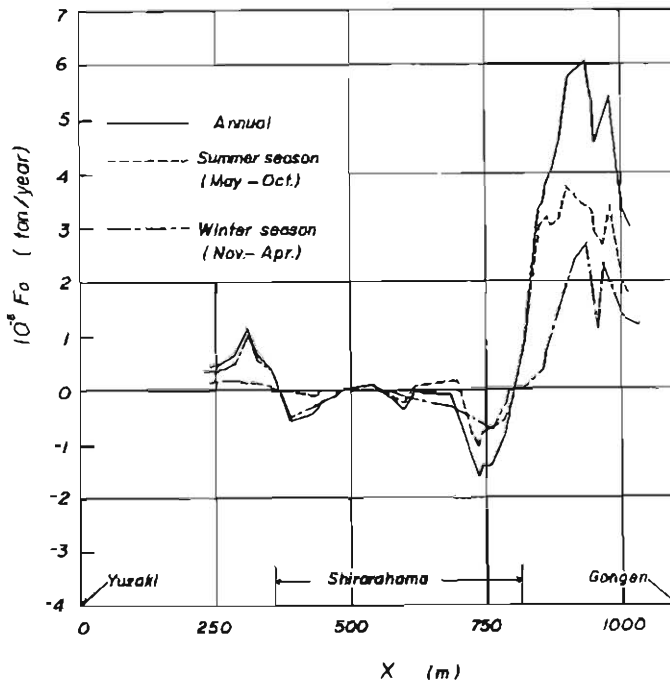


Fig. 29. Longshore distribution of annual and seasonal wave energy fluxes.

The short-term change of the distribution of the wave energy flux in Shirarahama beach is considered. The longshore distribution of the wave energy flux due to the incoming waves associated with the typhoon 7520 of which wave characteristics are shown in Fig. 5 is shown in Fig. 30. The total wave energy flux during the period of the storm has two negative peaks within the range of the beach and decreases to zero at the both ends of the beach, so that the characteristics are similar to the long-term ones in the winter season. Attempts in classifying hourly varying features of the wave energy flux can be concentrated in the interesting behavior at the both ends. These features are shown in Fig. 31 in every eight hours from 0:00 on 22nd until 16:00 on 24th September, 1975. At the time of 0:00 on 22nd, as shown in Fig. 31(a), the southward wave energy flux was produced in the range from the central part to the northern part of the beach, but decreased to zero at the both ends, whereas the northward wave energy flux did not decrease to zero at the north end at 8:00 and 16:00 on 22nd of the month. At 0:00 and 8:00 on 23rd, the northward wave energy flux intruded from the south end to the central part and decreased to zero at the northern end. Moreover, at 16:00 on 23rd the waves from the west direction directly attacked the central part, so that the wave energy flux suddenly changed with the distance and became finite at the northern end. Since wave periods and directions were nearly same for the period from 8:00 on 22nd to 8:00 on 23rd as shown in Fig. 5, it is considered that the change of the wave breaking point due to hourly variation of the wave heights may have influenced the change of the wave energy flux at the both ends. From these considerations it is found that when high waves associated with typhoons attack the beach, the distribution of the wave energy flux changes hourly according to the variation of wave characteristics, especially under a certain wave condition the wave energy flux does not decrease to zero at the end of Shirarahama beach. This fact may be one of the main causes of the recent beach erosion.

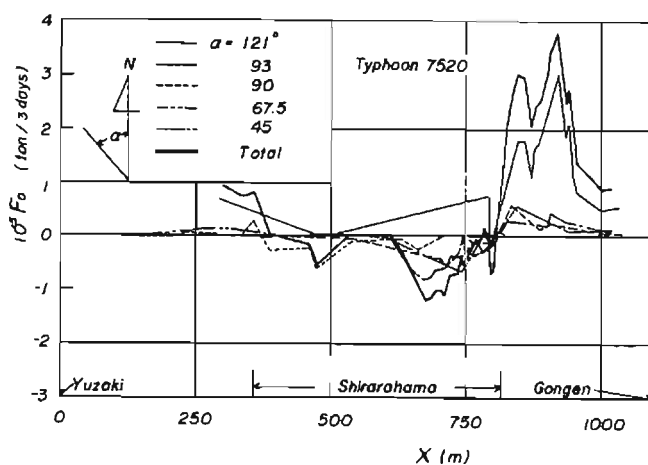


Fig. 30. Longshore distribution of wave energy flux of incoming waves associated with typhoon 7520.

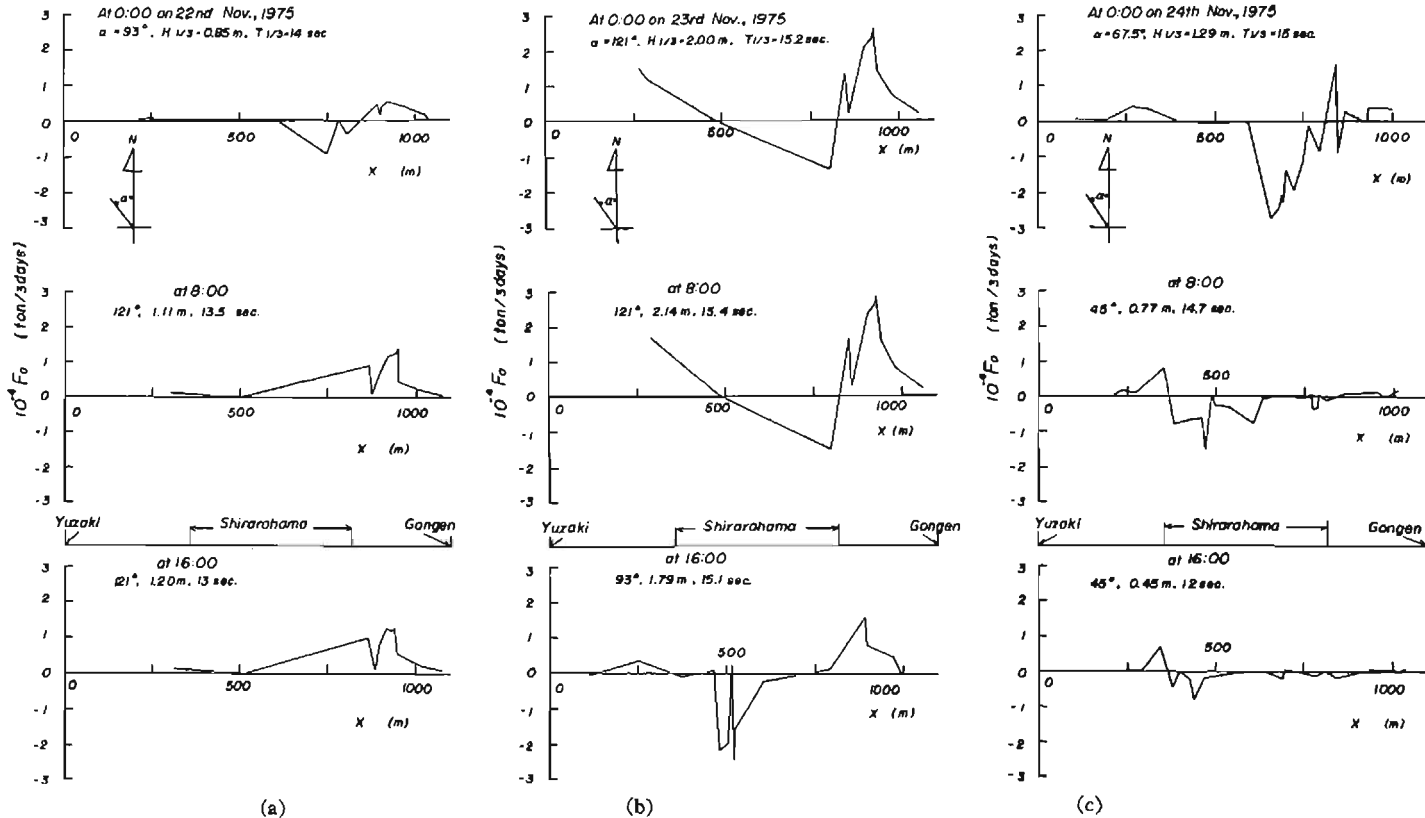


Fig. 31. Changes in longshore distribution of wave energy flux of incoming waves associated with typhoon 7520.

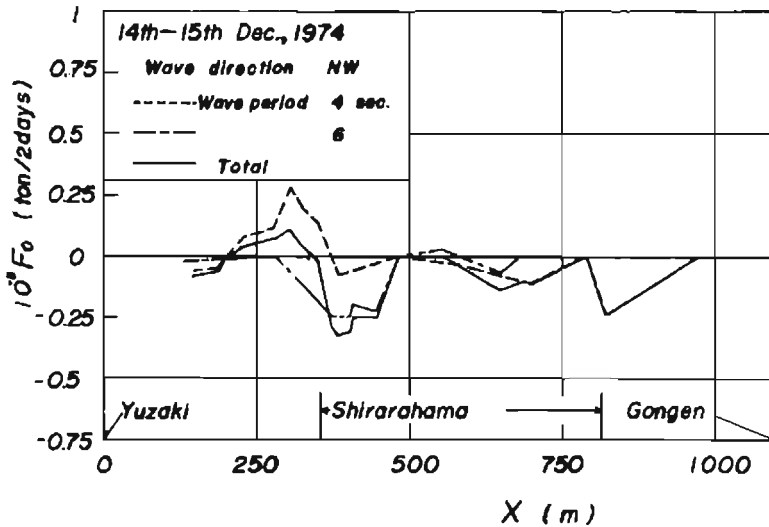


Fig. 32. Longshore distribution of wave energy flux of incoming waves associated with monsoon.

Another example of the short-term change of the wave energy flux is due to one of the typical stormy waves, which was associated with the northwest monsoon from 14th to 15th December, 1974, as shown in Fig. 6. The longshore distribution of the wave energy flux is shown in Fig. 32. The direction of the wave energy flux is reversed at the south end of the beach, owing to different wave periods, whereas the total one has a tendency similar to those in the long-term variation mentioned already. A series of the distributions of the wave energy flux in every four hours are shown in Fig. 33, as was done in Fig. 31. It is seen that a lot of the southward wave energy flux is produced by waves higher than one meter in wave height at the southern part and this may be one of the main causes of the beach erosion in the winter season.

## 5.2 Prediction of Beach Change

One of the most important aspects of a beach is its dynamic behavior responding to ever-changing wave action. In this section, firstly an outline of the mechanics of beach change with littoral drift is reviewed. The prediction of beach change of Shirarahama beach is considered based on the wave energy flux approach described already.

### (1) Outline of mechanics of beach change

The basic equations of beach change may consist of the equation of continuity of beach change and the equation of littoral drift, that is, the law of littoral drift. To analyze mathematically the beach change by waves, the basic equations should be solved together with a set of initial and boundary conditions. An outline of the mechanics of beach change which were originally proposed by Iwagaki<sup>3)</sup> follows.

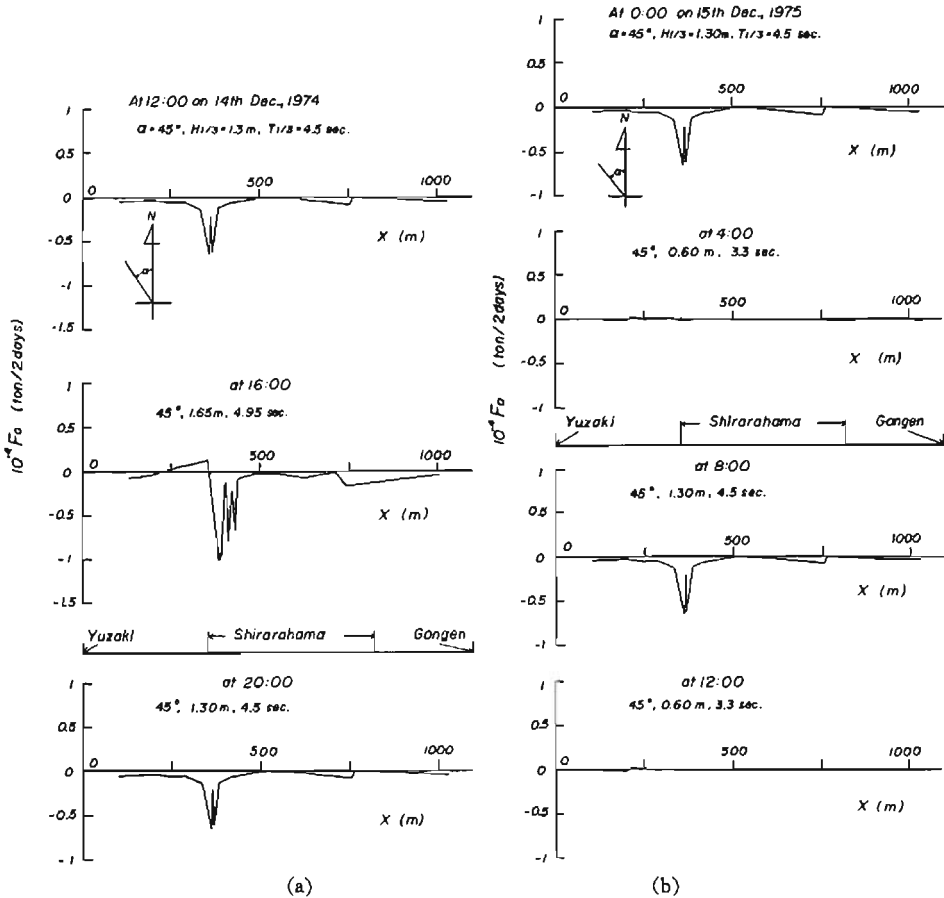


Fig. 33. Changes in longshore distribution of wave energy flux of incoming waves associated with monsoon.

According to the coordinate system shown in Fig. 34, the two dimensional continuity equation of beach change can be expressed as

$$\frac{\partial z}{\partial t} + \frac{1}{(1-\lambda)} \left( \frac{\partial q_x}{\partial x} + \frac{\partial q_y}{\partial y} \right) = 0 \quad (11)$$

in which  $q_x$  and  $q_y$  are the components of the rate of littoral sand drift in the  $x$  and  $y$  directions respectively. In a general case, the onshore-offshore sand transport associated with changes of beach profile is important, but a one dimensional approach to the beach change due to the longshore sand transport is herein described. Following the integration of Eq. (11) with respect to the offshore coordinate  $y$  by Iwagaki, the equation of continuity in the one-dimensional approach can be expressed with some modification by Tsuchiya<sup>9)</sup> as

$$\frac{h_b}{B} \frac{\partial y_p}{\partial t} = \frac{\partial \bar{h}}{\partial t} - \frac{h_b}{B} \left( 1 - \frac{\bar{h}}{h_b} \right) \frac{\partial B}{\partial t} - \frac{1}{(1-\lambda)B} \frac{\partial Q_x}{\partial x} + \frac{1}{B^2} Q_R(t) \delta(x-x_0) \quad (12)$$



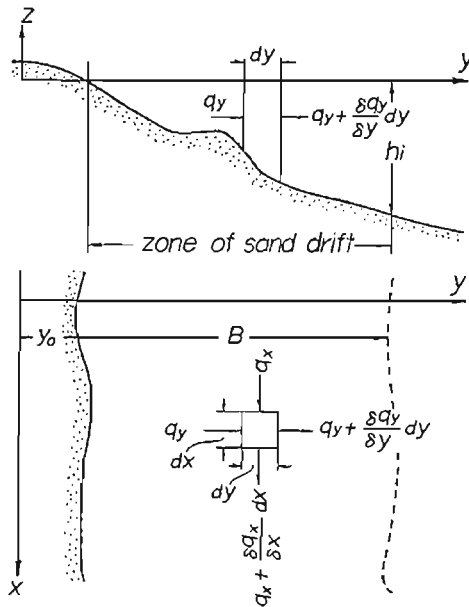


Fig. 34. Schematic diagram of beach change and coordinate system.

in which  $\bar{h}$  is the mean water depth,  $h_c$  the critical water depth for the threshold of sediment movement by waves,  $B$  is the width of the zone of drifting, and  $Q_R$  the sediment input from a river at  $x=x_0$ . According to Eq. (12), the following four main causes can be pointed out in the case of beach erosion, as already stated by Iwagaki. 1) Change of the beach profile in terms of  $\partial \bar{h} / \partial t$  2) Change of the critical water depth in terms of  $\partial h_c / \partial t$  3) Non-uniformity of the rate of littoral sand transport in terms of  $\partial Q_L / \partial x$  and 4) Change of the sediment source from a river in terms of  $Q_R(t) \delta(x-x_0)$ . In the case of long-term beach changes, it may be adequate for practical purposes to consider the effects of the third and fourth.

As already mentioned, a linear relation between the longshore wave energy flux and the rate of littoral sand drift has been confirmed, so that the beach change may be considered on the basis of the non-uniformity of the rate of littoral sand drift along the beach by the longshore distribution of the wave energy flux, because the sources of beach sediment from the Teratani river has been nearly exhausted in Shirarahama beach.

(2) Prediction of beach change

A schematic diagram of the long-term beach change is shown in Fig. 35, which may be associated with the longshore distributions of the wave energy flux along the beach. When the wave energy flux changes along the shoreline, the shoreline responds by altering its curvature and orientation to correspond to the distributions. In this beach, the northwesterly storms during a winter season cause the shoreline change near its both ends and the southerly ones during a summer season near its north end.

From this point of view, a seasonal change of the beach can be shown in Fig. 36

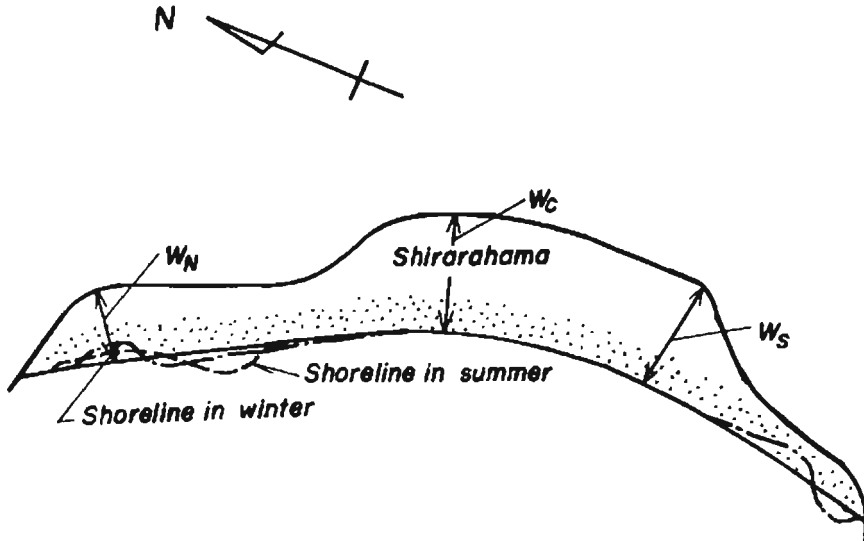


Fig. 35. Schematic diagram of seasonal change of shoreline.

which is expressed by the ratio  $W_N/W_S$  of the beach width at the northern and southern parts shown in Fig. 35. It is noted that this seasonal change can be explained by the qualitative prediction mentioned above. The ratio of  $W_S$  to  $W_C$  in winter defined in Fig. 35 is nearly equal to that in summer. Moreover, as expected in Fig. 29, there is no net longshore sand transport at the downdrift ends of the beach, and therefore it may be called as a closed sand drift system. The seasonal shoreline

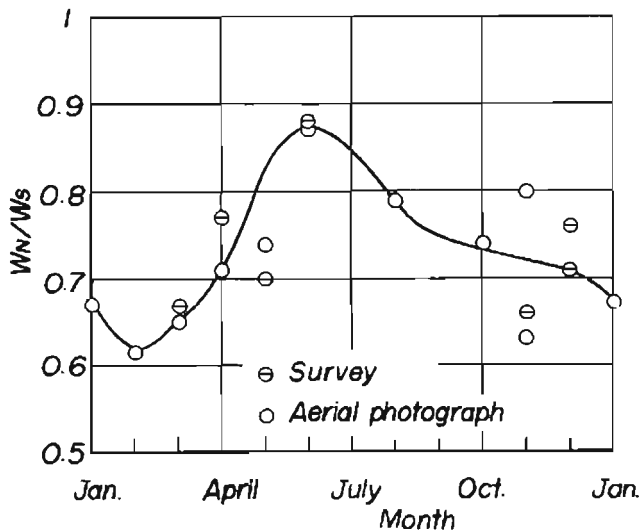


Fig. 36. Monthly change of beach width.

change may also be explained by the change in the bottom topography. A diagram of erosion and accretion of the sea bottom in Kanayama bay is shown in Fig. 11. In the period of this surveying, the typhoon 7220 struck Shionomisaki directly which is located at the southern end of the Kii peninsula and then took a course of the north-northwest direction. It is therefore considered that the high waves come to Kanayama bay from the south to the west wave direction. It is found that the erosion occurs in the southern area of the bay and the accretion does near the north end of the beach. The characteristics of the erosion and accretion near the Gongenzaki and Yuzaki headlands are not made clear, because of poor accuracy of the sounding near two headlands due to the submerged rocks. The seasonal changes may be restricted within the region of sandy beach. As already pointed out, because net loss of the beach sediment is negligibly small, it may be considered to be a beach in equilibrium.

The short-term beach change of Shirarahama beach is considered. High waves resulting from varying winds associated with typhoons and monsoons generate the outward net energy flux beyond the beach. As described already, because of no total wave energy flux for the period of typhoons and monsoons at the both ends, the inward wave energy flux should be equal to the outward one. As far as making the assumption that the longshore sand transport is proportional to the longshore wave energy flux, the budget of sand drift in the beach should be zero in relation to the short-term changes as well as long-term seasonal changes. However, the bottom topography near the Yuzaki and Gongenzaki headlands is so irregular, that the beach sediment is captured in submarine holes and some of them funnel out probably to very deep water off these headlands. Under this particular condition, the movement of the beach sediment at the ends tend to be one way transportation of sediment in the offshore direction, as it were one of the irreversible systems. Consequently, a little loss of the beach sediment from the end of Shirarahama beach in a short period of storm waves may govern its beach processes.

It is therefore concluded that the shoreline of Shirarahama beach wobbles according to the seasonal difference in the distributions of the wave energy flux, but may keep an equilibrium state for most of the whole year, whereas hourly varying intense wave action due to typhoons and monsoons causes the net loss of beach sediment and the gradual erosion for a short period of storm waves.

## 6. Conclusions

As the first report of a series of the investigations of pocket beaches, part of the recent field studies of the beach processes of Shirarahama "a pocket beach" is described. The main conclusions can be summerized as follows

- 1) In Shirarahama beach, there are two typical changes in the beach processes caused by blown sands owing to strong winds in monsoon seasons and by sand drift owing to high waves and nearshore currents associated with typhoons and monsoons.
- 2) It is concluded that the main source of the beach sediment is the hinterland, especially the Teratani river, but it has been exhausted due to the recent urbanization

This fact is confirmed by the offshore distribution of the median diameter, standard deviation of the beach and bottom sediment in Kanayama bay, and their mineral composition.

3) It is found from the detailed sampling of the beach sediment that the median diameter and standard deviation of the sediment are rhythmically distributed on the swash area and this fact may be due to the swash transport as well as characteristics of the beach cusps.

4) Beach changes severely occur by blown sands in the winter season. A one-dimensional approach for the prediction of the beach change is proposed on the basis of both the law of sediment transport and the equation of continuity for beach changes. It is concluded from the comparison between the predicted and observed beach changes that this method of prediction is applicable with satisfactory agreement between them for practical purposes.

5) The distribution of the longshore wave energy flux along the shoreline instead of the total rate of sand drift is considered to find a long-term beach change. It is concluded that the beach is stable from the point of view of such a long-term beach change. It is however found from the hourly changes in the distribution of the longshore wave energy flux that the beach sediment may be transported at the both ends of the beach for a very short period in high waves associated with typhoons and monsoons.

### Acknowledgements

Part of this research was supported by the Science Funds of the Ministry of Education, under Grant No. 285119. The authors thank Messrs. S. Hayashi and Y. Kameyama for their kind co-operation in conducting this field investigation and Miss Y. Hajika for kind help in typing this manuscript.

### References

- 1) Silvester, R.: Headland defense of coasts, Proc. 15th Conf. on Coastal Eng., 1976, pp. 1394-1406.
- 2) Toyoshima, O.: Design of a detached breakwater system, Proc. 14th Conf. on Coastal Eng., 1974, pp. 1419-1431.
- 3) Horikawa, K. and H. W. Shen: Sand movement by wind action, — on the characteristics of sand traps —, Beach Erosion Board, Tech. Memo. No. 119, 1960.
- 4) Tsuchiya, Y and Y. Kawata: On the law of sediment transport by winds by means of saltation of sand grains, Proc. 19th Conf. on Hydraulics, JSCE, 1975, pp.7-12 (in Japanese).
- 5) Komar, P. D.: Beach sand transport, distribution and total drift, Proc. ASCE, Vol. 103, No. WW2, 1977, pp. 225-239.
- 6) Tsuchiya, Y. and T. Yasuda: A theoretical model of prediction of beach changes, Proc. 25th Conf. on Coastal Eng., JSCE, 1978, pp. 167-171 (in Japanese).
- 7) Worthington, H. W. and J. B. Herbich: A computer program to estimate the combined effect of refraction and diffraction of water waves, Sea Grant Pub., Texas A & M Univ., No. 219, 1970, pp. 57.
- 8) Iwagaki, Y.: Beach erosion, Text Book for Summer Seminar in Hydraulic Engineering, JSCE, 1966, pp. B-17-1-17 (in Japanese).
- 9) Tsuchiya, Y.: Beach sediment balance and beach change, Text Book for Summer Seminar in Hydraulic Engineering, JSCE, 1973, pp. B-3-1-19 (in Japanese).
- 10) Coastal Engineering Research Center: Shore protection manual, US Army, 1973.